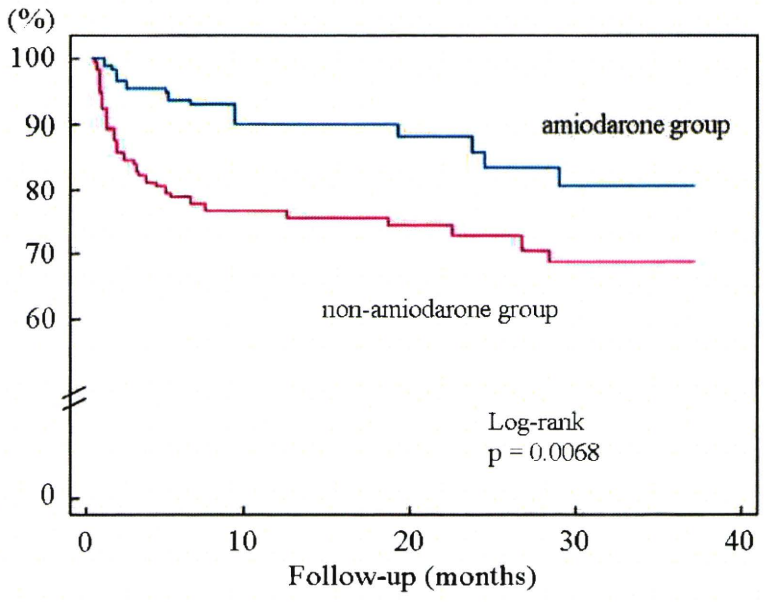

Figure. Event-free curve of inappropriate implantable cardioverter defibrillator therapy. Kaplan-Meier plots depicting the cumulative risk of inappropriate therapies. The event-free survival was better among the patients treated with amiodarone.

Table 2. Causes of Inappropriate Therapies

	Amiodarone group	Non-amiodarone group	P value
Sinus tachycardia, n (%)	6 (5)	13 (11)	NS
Atrial fibrillation, n (%)	3 (3)	14 (12)	0.0098
Atrial flutter, n (%)	1 (1)	1 (1)	NS
NSVT, n (%)	2 (2)	1 (1)	NS
Sensing failure, n (%)	1 (1)	1 (1)	NS
Lead failure, n (%)	0 (0)	1 (1)	NS
EMI, n (%)	1 (1)	0 (0)	NS
Inappropriate shock/ATP, n	10/4	16/15	NS

Data are number of subjects (%).
NSVT, nonsustained ventricular tachycardia; EMI, electromagnetic interference; ATP, antitachycardia pacing.

Results

Patient Characteristics

The baseline characteristics of the patients are summarized in Table 1. There were no significant differences between the 2 groups in terms of sex, age, New York Heart Association functional class, prior pacemaker implantation or history of supraventricular tachyarrhythmias. The prevalence of ischemic heart disease was higher in the amiodarone group than in the non-amiodarone group (47 vs 33%, P=0.044). The patients in the amiodarone group had a lower left ventricular ejection fraction (31±12% in the amiodarone group, 40±17% in the non-amiodarone group; P<0.0001), larger left atrial diameter (43±10 mm in the amiodarone group, 40±9 mm in the non-amiodarone group; P=0.026), and smaller total number of heart beats on the 24-h Holter monitoring (88,157± 16,536 beats in amiodarone group, 93,463±18,199 beats in the non-amiodarone group; P=0.049). Dual-chamber ICDs were more frequently implanted in the patients in the amiodarone group as compared with those in the non-amiodarone group (47% in the amiodarone group, 22% in the non-amiodarone group, P=0.0001). There was no significant difference in the combined use of β-blockers. The mean daily maintenance dose of amiodarone was 170±52 mg (range, 50–400 mg) in the amiodarone group. Although no fatal side-effects were observed during the follow-up, amiodarone was discontinued because of adverse drug effects in 19 patients (16%), including thyroid dysfunction in 11 (9%), pulmonary intoxication in 6 (5%), liver dysfunction in 1 (0.9%), and proarrhythmic effects in 1 (0.9%).

Incidence and Cause of Inappropriate ICD Therapies

In total, 14 patients (12%) in the amiodarone group and 31 (27%) in the non-amiodarone group had at least 1 inappropriate therapy during a mean follow-up of 29±21 months. Event-free curves were computed for the 2 groups using the Kaplan-Meier method (Figure). The inappropriate therapies occurred less frequently in the amiodarone group than in the non-amiodarone group (P=0.0068 by log-rank test). The proportion of patients receiving at least 1 inappropriate shock delivery was 71% in the amiodarone group, and 52% in the non-amiodarone group. As a cause of the inappropriate therapies, only AF was significantly frequent in the non-amiodarone group (3 of 116 patients, 3% in the amiodarone group, 14 of 116 patients, 12% in the non-amiodarone group; P= 0.0098) (Table 2). There was no history of AF documenta-

Table 3. Univariate Analysis of the Inappropriate Therapies

	Inappropriate therapy		P value
	Yes (n=45)	No (n=187)	
M/F	36/9	146/41	NS
Age ≥65 years	11 (24)	69 (37)	NS
NYHA class III or IV, n (%)	2 (4)	13 (7)	NS
Ischemic heart disease, n (%)	16 (36)	76 (41)	NS
Atrial fibrillation, n (%)			
Paroxysmal or persistent, n (%)	16 (36)	24 (13)	0.0007
Permanent, n (%)	6 (13)	16 (9)	NS
LVEF, %	38±15	35±16	NS
LAD, mm	41±9	41±10	NS
Dual chamber, n (%)	17 (38)	64 (34)	NS
Class Ia, n (%)	0 (0)	8 (4)	NS
Class Ib, n (%)	10 (22)	41 (22)	NS
Amiodarone, n (%)	14 (31)	102 (55)	0.0079
Sotalol, n (%)	2 (4)	8 (4)	NS
β-blocker, n (%)	26 (58)	105 (56)	NS

Data are number of subjects (%).
Abbreviations as in Table 1.

tion before ICD implantation in 5 of 14 patients with inappropriate therapies in the non-amiodarone group. On the other hand, all patients in the amiodarone group with inappropriate therapies caused by AF had a history of spontaneous AF before ICD implantation.

Predictors of Inappropriate ICD Therapies

The results of the univariate analysis for inappropriate ICD therapies are shown in Table 3. A history of spontaneous AF before ICD implantation and no administration of amiodarone were associated with an increased risk of an inappropriate therapy. The administration of β-blockers or sotalol, and dual-chamber ICD implantation did not differ statistically between those with and without inappropriate therapies. The multivariate logistic regression analysis showed that amiodarone therapy (odds ratio (OR) 0.38, 95% confidence interval (CI) 0.19–0.77, P=0.0073) and absence of preexisting spontaneous (paroxysmal/persistent) AF (OR 0.27, 95%CI 0.13–0.57, P=0.0007) remained as independent predictors of a lower risk of inappropriate therapies (Table 4).

Table 4. Multivariate Logistic Regression Analysis of the Inappropriate Therapies

	Odds ratio	95%CI	P value
Amiodarone	0.38	0.19–0.77	0.0073
Free from PAF	0.27	0.13–0.57	0.0007

PAF, paroxysmal or persistent atrial fibrillation; CI, confidence interval.

Discussion

Major Findings

In this study, we demonstrated that a history of paroxysmal or persistent AF was a major factor in the delivery of inappropriate therapy by an ICD in patients with structural disease. We further demonstrated that the administration of amiodarone concomitant with implantation of an ICD was associated with less inappropriate ICD deliveries.

Amiodarone as an Adjunctive Therapy With ICDs

The aim of adjunctive drug therapy with ICDs is to reduce both the number of appropriate shocks triggered by ventricular tachyarrhythmias and to prevent inappropriate shocks because of SVTs. The avoidance of frequent shocks through the use of antiarrhythmic agents may be crucial for the safety and QOL of patients with ICDs.

Amiodarone, which prolongs the action potential duration and refractoriness of cardiac tissue, has emerged as the antiarrhythmic agent of choice for treating life-threatening ventricular arrhythmias. Previous prospective randomized studies have suggested that amiodarone prevents the recurrence of VT/VF and unexpected death, and reduces the total mortality in patients with ventricular tachyarrhythmias. Recently, we reported the usefulness of amiodarone therapy guided by VT inducibility for preventing VT/VF recurrence in patients with structural heart diseases and relatively preserved left ventricular ejection function (≥30%).[16] On the other hand, the combined use of antiarrhythmic agents with ICDs might lead to adverse responses such as an unacceptable increase in the DFT, underdetection of VT/VF because of prolongation of the arrhythmia cycle length beyond the programmed detection interval or potential proarrhythmias or extracardiac toxicity. Amiodarone is widely used as an adjuvant drug therapy with ICDs; however, there have been few randomized placebo–control trials to evaluate whether amiodarone is beneficial or not.

The efficacy of combination therapy with oral amiodarone plus β-blockers in patients receiving a dual-chamber ICD for secondary prevention has been prospectively evaluated in a randomized multicenter trial,[13] which compared both amiodarone plus β-blockers and sotalol with standard β-blocker therapy for the prevention of ICD shocks in patients with an ejection fraction ≤40% and spontaneous or inducible ventricular tachyarrhythmias and confirmed the efficacy of amiodarone plus β-blockers for avoiding both excessive appropriate and inappropriate shocks without significantly increasing the risk of treatment related mortality. Recently, amiodarone alone also has been shown to be effective for avoiding inappropriate ICD therapies in a patient with AF and congestive heart failure.[14,15] Our study evaluated inappropriate ICD ther-

apies, including not only shock therapies but also antitachycardia pacing therapies, from either single- or dual-chamber ICD systems in patients with and without the oral administration of amiodarone, and our reaults suggest that not using amiodarone was associated with a higher risk of inappropriate therapies in patients with organic heart disease, regardless of β-blocker administration.

Effect of Amiodarone on Inappropriate ICD Therapies

In the present study, only AF was a significant independent cause of inappropriate therapies in a comparison of patients with and without amiodarone. The incidence of inappropriate therapies caused by AF was 2.6% and 12.1%, respectively. Interestingly, half of those patients received inappropriate therapies because of newly developed AF in patients without amiodarone. Further, no cases of inappropriate therapies caused by newly developed AF were observed in the amiodarone group. The patients implanted with an ICD usually have structural heart disease with impaired LV function. There is increased LV end-diastolic pressure caused an increased left atrial pressure from nearly 15–25% and greater complications of AF in these patients.[1,5–7] The reduction in the incidence of spontaneous AF is most likely 1 of the mechanisms of the reduction in inappropriate therapies by ICDs with adjunctive amiodarone. The effect of amiodarone in preventing newly developed AF has been widely recognized.[17,18] Singh et al showed the effectiveness of amiodarone in preventing new AF in patients with sinus rhythm at baseline and reported that ICD shocks were more often seen in patients with AF.[19] Amiodarone also has a β-blocker-like effect and decreases the heart rate during sinus rhythm or AF.[20] However, in the present study it was not possible to clarify whether amiodarone could reduce the frequency of spontaneous AF or decrease the heart rate during AF by its negative chronotropic effects.

Study Limitations

First, this was a retrospective, single-center study and lacked the clear advantage of a multicenter prospective, randomized study. The OPTIC trial suggested that amiodarone and β-antagonists could prevent inappropriate ICD therapy and our study has emphasized that result. However, β-blocker use was only 44% in a large cohort study in Japan,[21] indicating it is not frequently administered in the Japanese patient population with structural heart disease and ICD implantation. We could not confirm the reason for the relatively lower use of β-blockers in our study. One possible reason is that we included patients who underwent ICD implantation at the end of the 90 s (from 1990 to 2005) and β-blockers might be not have been frequently used during that time. Second, the patients in the amiodarone group were more likely to have decreased cardiac function and a larger left atrium. Therefore, amiodarone might have been prescribed for the sicker patients, leading to an underestimation of the drug effect. Third, the ratio of dual-chamber ICD systems was significantly higher in the amiodarone group, so it is possible that the AF-discriminating algorithms of the dual-chamber devices contributed to the reduced number of inappropriate therapies in the amiodarone group;[22] however, the ratio of dual-chamber ICDs did not statistically differ between those with and without inappropriate therapies. Fourth, there was a tendency to a higher incidence of inappropriate therapy because of sinus tachycardia in the non-amiodarone group (P<0.10). Amiodarone may also contribute to reducing sinus rate. A previous study supported that amiodarone can reduce the sinus rate.[20] In fact, patients in the amiodarone group had a smaller total number of heart beats on 24-h Holter monitoring (P=0.049) in our study. However, sinus rate did not reach statistical significance as a cause of inappropriate therapy.

Conclusions

This study demonstrated that inappropriate ICD therapies occur predominantly in patients with spontaneous AF and structural heart disease. The results also suggest that amiodarone therapy may be associated with a lower rate of inappropriate ICD therapies safely under careful observation.

Disclosure

No conflict of interest.

References

1. The Antiarrhythmics versus Implantable Defibrillators (AVID) Investigators. A comparison of antiarrhythmic-drug therapy with implantable defibrillators in patients resuscitated from near-fatal ventricular arrhythmias. *N Engl J Med* 1997; **337:** 1576–1583.
2. Connolly SJ, Gent M, Roberts RS, Dorian P, Roy D, Sheldon RS, et al. Canadian Implantable Defibrillator Study (CIDS): A randomized trial of the implantable cardioverter defibrillator against amiodarone. *Circulation* 2000; **101:** 1297–1302.
3. Kuck KH, Cappato R, Siebels J, Ruppel F, for the CASH Investigators. Randomized comparison of antiarrhythmic drug therapy with implantable defibrillators in patients resuscitated from cardiac arrest: The Cardiac Arrest Study Hamburg (CASH). *Circulation* 2000; **102:** 748–754.
4. Multicenter Automatic Defibrillator Implantation Trial Investigators. Improved survival with an implanted defibrillator in patients with coronary disease at high risk for ventricular arrhythmia. *N Engl J Med* 1996; **335:** 1933–1940.
5. Moss AJ, Zareba W, Hall WJ, Klein H, Wilber DJ, Cannom DS, et al. Prophylactic implantation of a defibrillator in patients with myocardial infarction and reduced ejection fraction. *N Engl J Med* 2002; **346:** 877–883.
6. Kadish A, Dyer A, Daubert JP, Quigg R, Estes NA, Anderson KP, et al. Prophylactic defibrillator implantation in patients with nonischemic dilated cardiomyopathy. *N Engl J Med* 2004; **350:** 2151–2158.
7. Bardy GH, Lee KL, Mark DB, Poole JE, Packer DL, Boineau R, et al. Amiodarone or an implantable cardioverter-defibrillator for congestive heart failure. *N Engl J Med* 2005; **352:** 225–237.
8. Schron EB, Exner DV, Yao Q, Jenkins LS, Steinberg JS, Cook JR, et al. Quality of life in the antiarrhythmics versus implantable defibrillators trial: Impact of therapy and influence of adverse symptoms and defibrillator shocks. *Circulation* 2002; **105:** 589–594.
9. Carroll DL, Hamilton GA. Quality of life in implanted cardioverter defibrillator recipients: The impact of a device shock. *Heart Lung* 2005; **34:** 169–178.
10. Herrmann C, von zur Muhen F, Schaumann A, Buss U, Kemper S, Wantzen C, et al. Standardized assessment of psychological well-being and quality of life in patients with implanted defibrillators. *Pacing Clin Electrophysiol* 1997; **20:** 95–103.
11. Theuns DA, Klootwijk AP, Simoons ML, Jordaens LJ. Clinical variables predicting inappropriate use of implantable cardioverter-defibrillator in patients with coronary heart disease or nonischemic dilated cardiomyopathy. *Am J Cardiol* 2005; **95:** 271–274.
12. Nanthakumar K, Dorian P, Paquette M, Greene M, Edwards J, Heng D, et al. Is inappropriate implantable defibrillator shock therapy predictable? *J Interv Card Electrophysiol* 2003; **8:** 215–220.
13. Connolly SJ, Dorian P, Roberts RS, Gent M, Bailin S, Fain ES, et al. Comparison of beta-blockers, amiodarone plus beta-blockers, or sotalol for prevention of shocks from implantable cardioverter defibrillators: The OPTIC Study: A randomized trial. *JAMA* 2006; **295:** 165–171.
14. Satomi K, Kurita T, Takatsuki S, Yokoyama Y, Chinushi M, Tsuboi N, et al. Amiodarone therapy in patients implanted with cardioverter-defibrillator for life-threatening ventricular arrhythmias. *Circ J* 2006; **70:** 977–984.
15. Lee CH, Nam GB, Park HG, Kim HY, Park KM, Kim J, et al. Effects of antiarrhythmic drugs on inappropriate shocks in patients with implantable cardioverter defibrillators. *Circ J* 2008; **72:** 102–105.

16. Aiba T, Yamagata K, Shimizu W, Taguchi A, Satomi K, Noda T, et al. Electrophysiologic study-guided amiodarone for sustained ventricular tachyarrhythmias associated with structural heart diseases. *Circ J* 2008; **72:** 88–93.
17. AFFIRM First Antiarrhythmic Drug Substudy Investigators. Maintenance of sinus rhythm in patients with atrial fibrillation: An AFFIRM substudy of the first antiarrhythmic drug. *J Am Coll Cardiol* 2003; **42:** 20–29.
18. Kochiadakis GE, Igoumenidis NE, Marketou ME, Solomou MC, Kanoupakis EM, Vardas PE. Low-dose amiodarone versus sotalol for suppression of recurrent symptomatic atrial fibrillation. *Am J Cardiol* 1998; **81:** 995–998.
19. Singh SN, Poole J, Anderson J, Hellkamp AS, Karasik P, Mark DB, et al. Role of amiodarone or implantable cardioverter/defibrillator in patients with atrial fibrillation and heart failure. *Am Heart J* 2006; **152:** 974.e7–e11.
20. Nul DR, Doval HC, Grancelli HO, Varini SD, Soifer S, Perrone SV, et al. Heart rate is a marker of amiodarone mortality reduction in severe heart failure: The GESICA-GEMA Investigators [Grupo de Estudio de la Sobrevida en la Insuficiencia Cardiaca en Argentina-Grupo de Estudios Multicéntricos en Argentina]. *J Am Coll Cardiol* 1997; **29:** 1199–1205.
21. Satomi K, Kurita T, Takatsuki S, Yokoyama Y, Chinushi M, Tsuboi N, et al. Amiodarone therapy in patients implanted with cardioverter-defibrillator for life-threatening ventricular arrhythmias. *Circ J* 2006; **70:** 977–984.
22. Friedman PA, McClelland RL, Bamlet WR, Acosta H, Kessler D, Munger TM, et al. Dual-chamber versus single-chamber detection enhancements for implantable defibrillator rhythm diagnosis: The detect supraventricular tachycardia study. *Circulation* 2006; **113:** 2871–2879.

EUROPEAN SOCIETY OF CARDIOLOGY®

Europace (2010) **12**, 719–725
doi:10.1093/europace/euq067

The positional relationship between the coronary sinus musculature and the atrioventricular septal junction

Taka-aki Matsuyama[1]*, Hatsue Ishibashi-Ueda[1], Yoshihiko Ikeda[1], Yuko Yamada[2], Hideo Okamura[2], Takashi Noda[2], Kazuhiro Satomi[2], Kazuhiro Suyama[2], Wataru Shimizu[2], Naohiko Aihara[2], Shiro Kamakura[2], and Shin Inoue[3]

[1]Department of Pathology, National Cardiovascular Center, 5-7-1 Fujishirodai Suita-City, 565-8565 Osaka, Japan; [2]Division of Cardiovascular Medicine, Department of Internal Medicine, National Cardiovascular Center, Osaka, Japan; and [3]Department of Internal Medicine, Showa University Dental Hospital, Tokyo, Japan

Received 21 December 2009; accepted after revision 10 February 2010; online publish-ahead-of-print 12 March 2010

Aims The atrioventricular (AV) septal junction includes the coronary sinus (CS) and the compact part of the AV node and its posterior extensions. It has been recognized as the target site for ablation therapy of the AV nodal reentrant tachycardia and its variant forms. Despite the clinical significance of this region, the arrangement of the musculature in the AV septal junction, including the CS, has not fully been elucidated. We tried to explore the histological muscular diversity within the AV septal junction.

Methods and results Sixteen autopsied human hearts (seven women), mean age 59.8 years, without structural anomalies, were studied. We removed the whole AV septum, including the CS opening after the macroscopic measurements, and prepared serial sections parallel to mitral and tricuspid annuli (short-axis style) to elucidate the positional relationships between the compact AV node and the CS musculature. Out of 16 hearts, the CS musculature extended deeply into the AV septal junction in eight hearts. In the other eight hearts, the CS musculature was located above the AV septal junction. In the former group, we found that the offset of both annuli was wide (mean 3.8 ± 1.4 vs. 2.4 ± 1.1 mm), the distance between CS opening and membranous septum was long (mean 14.8 ± 1.6 vs. 12.3 ± 2.2 mm), and the CS opening level was lower and closer to the His bundle level (mean 2.8 ± 1.9 vs. 5.8 ± 2.9 mm) ($P < 0.05$).

Conclusion The deep extension of CS musculature into the AV septal junction seems to increase the tissue non-uniformity in this area.

Keywords Atrioventricular node • Coronary sinus • Histology • Atrioventricular nodal reentrant tachycardia • Atrioventricular septal junction

Introduction

The Koch's triangle is known as a landmark of the atrioventricular (AV) nodal tissue.[1] It is observed from the macroscopic endocardial view of the right atrium, and is delineated by the following three elements: the tendon of Todaro, the tricuspid valve annulus, and the coronary sinus (CS) opening. In a study, it was shown that the dimensions of the Koch's triangle show considerable diversity.[2] In addition to this diversity, the myocardial orientation beneath the endocardium has not fully been elucidated. However, the recent advances of clinical electrophysiology revealed that most of the critical regions of the AV nodal reentrant tachycardia (AVNRT) prevail around the anterior CS opening,[3] though the histological prospects of the pathway of AVNRT are still obscure.[4] Therefore, we propose a modified histological method that can provide a reference for the relation between the dimensions of Koch's triangle and the arrangement of CS musculature within the AV septal junction.

* Corresponding author. Tel: +81 6 6833 5012; fax: +81 6 6833 9865, Email: takamatu@hsp.ncvc.go.jp

Published on behalf of the European Society of Cardiology. All rights reserved. © The Author 2010. For permissions please email: journals.permissions@oxfordjournals.org.

Methods

Subjects

The present study included randomly selected 16 autopsied human hearts (9 men, 7 women) without structural anomalies or a history of significant conspicuous supraventricular arrhythmia. The mean age was 57.9 ± 18.2 years ranging between 20 and 80 years. Ten of the human subjects died of malignant diseases, the others died of a liver disease, sepsis, pneumonia, brain haemorrhage, aortic aneurysm, or gastrointestinal bleeding. None of them died of structural heart disease.

Macroscopic measurement

After fixation in 10% formalin, the posterior AV septal junction, including the opening of the CS, tricuspid valve, and mitral valve, was removed en bloc. We defined the CS as the portion that begins at the confluence of the great cardiac vein and the oblique vein (bundle) of Marshall and ends with its ostium in the right atrium (CS opening).[5] We measured each dimension in this area as follows: (a) the width of the mitral valve-tricuspid valve offset, (b) the longitudinal distance between the CS opening and membranous septum (CS-MS offset), (c) the diameter and the surface area of the CS opening, (d) the distance between the CS opening and tricuspid valve annulus (septal isthmus), and (e) the distance between CS opening and membranous septum (*Figure 1*).

Microscopic observation

Removed blocks of the hearts were conventionally processed to paraffin inclusions, and then serial sections of 7-μm thickness were made parallel to both the tricuspid and mitral valve annuli, i.e. the short-axis plane of the both ventricles. From the level of the tricuspid valve to the posterior margin of CS opening, every 10th section was stained with Masson's trichrome. We observed the distribution of the CS musculature in this area, and compared it with the dimensions of the Koch's triangle. The CS musculature was defined as the myocardial coverage of the CS.[6]

Statistical analysis

For all the study subjects, we compared heart weights, and each dimension within the Koch's triangle. The values were shown as mean ± SD. One-factor ANOVA was used for statistical comparisons between the groups. A *P*-value of <0.05 was considered statistically significant.

Results

Measurements

The mean heart weight was 334.9 ± 75.8 g, ranging between 169 and 465 g. The macroscopic measurements as described in *Figure 1* were as follows: (a) the mean width of the tricuspid valve–mitral valve offset was 3.1 ± 1.4 mm, (b) the mean longitudinal distance between the CS opening level and membranous septum level (CS–MS offset) was 4.3 ± 2.8 mm, (c) the mean surface area and diameter of the CS opening were 43.7 ± 17.3 mm^2 and 10.5 ± 2.8 mm, respectively, (d) the mean septal isthmus length was 9.9 ± 1.8 mm, (e) the mean distance between CS opening and membranous septum was 13.5 ± 2.3 mm. Detailed measurements and histological patterns of the each individual are shown in *Table 1*.

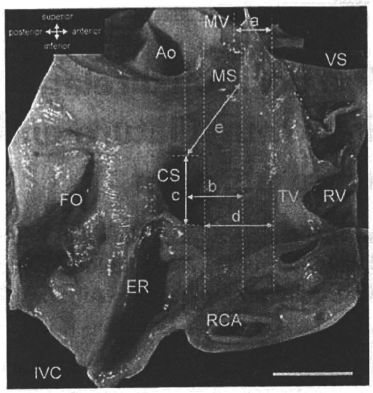

Figure 1 Macroscopic endocardial view of the Koch's triangle from the right atrium. Arrows shows the measured dimensions, (a) the width of the mirtal valve–tricuspid valve offset, (b) the longitudinal distance between the coronary sinus opening and membranous septum (CS-MS offset), (c) the diameter and the surface area of the coronary sinus opening, (d) the distance between the coronary sinus opening and tricuspid valve annulus (septal isthmus), and (e) the distance between coronary sinus opening and membranous septum. Tissue sections were sliced parallel to the dotted lines on the tricuspid valve annulus (short axis) in this photograph. Ao, aorta; CS, coronary sinus; ER, Eustachian ridge; FO, foramen ovale; IVC, inferior vena cava; MS, membranous septum; MV, mitral valve; RCA, right coronary artery; RV, right ventricle; TV, tricuspid valve; VS, ventricular septum. Bar = 10 mm.

Relationship of the distribution of coronary sinus musculature and the atrioventricular septal junction

We divided the hearts into two groups according to the distribution patterns of CS musculature.

Group A: deep extension group (*Figure 2*)

At a level just above the tricuspid valve, the CS musculature around the CS opening deeply intrudes into the AV septum and merges with the myocardium of the septal isthmus. In the middle part of the CS cavity, the CS musculature was found to have sparse and loose connections with the left atrial myocardium just beneath the compact AV node. In this group, the myocardial connections between both atria were observed mainly at the superior border of the CS opening through the CS musculature.

Group B: superficial extension group (*Figure 3*)

Sections within the septal isthmus just above both mitral and tricuspid annuli showed that the compact node was located between left and right atrial myocardium, and this configuration

Table 1 Macroscopic measurements and distribution patterns of the coronary sinus musculature into atrioventricular septum

No.	Age/sex	Heart weight (g)	a	b	c		d	e	Distribution pattern of CS musculature into AV septum
			TV-MV offset (mm)	CS-MS offset (mm)	CS opening size (mm^2)	CS opening diameter (mm)	CS-TV (mm)	CS-MS (mm)	
1	20/F	169	1.4	1	31.4	10	7	15	Group A
2	26/M	380	5.1	2	56.5	12	10	15	Group A
3	34/M	370	1.4	5	40.8	13	11	15	Group B
4	47/F	280	3.5	4	25.1	8	7	15	Group A
5	51/F	270	2.8	6	21.2	9	11	16	Group A
6	55/M	310	5.6	4	76.9	14	9	15	Group A
7	59/M	370	2.8	0	43.2	11	10	12	Group B
8	60/M	290	4.9	0	71.4	13	10	17	Group A
9	66/F	450	1.4	8	27.5	7	8	8	Group B
10	67/F	300	2.1	3	47.1	12	8	12	Group B
11	67/F	345	1.4	7	43.2	11	12	14	Group B
12	69/M	280	4.4	8	28.3	9	9	11	Group B
13	75/M	340	3.5	7	47.1	12	13	12	Group B
14	75/M	465	2.9	3	70.7	15	10	12	Group A
15	76/F	310	4.2	2	33.0	7	12	13	Group A
16	80/M	430	2.1	8	35.3	5	11	14	Group B
Mean ± SD	57.9 ± 18.2	334.9 ± 75.8	3.1 ± 1.4	4.3 ± 2.8	43.7 ± 17.3	10.5 ± 2.8	9.9 ± 1.8	13.5 ± 2.3	

AV, atrioventricular; CS, coronary sinus; MS, membranous septum; MV, mitral valve; TV, tricuspid valve; a-e, see *Figure 1*.

means that this level is above the AV septal junction and that the CS musculature does not deeply intrude into AV septum. Not only the CS musculature was found to have no connections with the left atrial myocacrdium in this level, but also myocardial connections between both atria were hardly observed.

In the middle part of the CS of this group, it was found that the musculature of the CS opening merges with the myocardium of the vestibule of the right atrium, in which it is defined as the flat endocardial sector just above the AV valve attachment (*Figure 3C*).[7] At this level, the CS musculature was close to the left atrial myocardium. The myocardial connections between both atria were observed mainly in the antero-superior border of CS opening through the CS musculature.

Comparison between the dimensions of each group

The CS musculature showed a deep extension distribution into the AV septal junction in eight hearts (Group A, *Figure 2*). The musculature around the CS opening spread beneath the level of the mitral valve annulus as shown in *Figure 2B*. The remaining eight hearts (Group B, *Figure 3*) showed that the CS musculature was located above the AV septal junction and showed non-intruding distribution, i.e. superficial extension. In Group A, the offset of both annuli was significantly wider (mean 3.8 ± 1.4 vs. 2.4 ± 1.1 mm, $P < 0.05$), the length between the CS opening and the membranous septum was longer (mean 14.8 ± 1.6 vs. 12.3 ± 2.2 mm, $P < 0.05$), and the CS opening level was lower and closer to the membranous septum level (His bundle level) (mean 2.8 ± 1.9 vs. 5.8 ± 2.9 mm, $P < 0.05$; *Table 2*).

Figure 4 represents a schematic explanation for the distributions of the CS musculature in both groups. In Group A (deep extension, *Figure 4A*), one normal variant of the tricuspid valve anatomy shows the downward displacement of the tricuspid valve annulus into the right ventricle, which draws the CS opening more anteriorly with constant distance between the tricuspid valve annulus and the CS opening. In this group, the CS is facing the compact AV node by its superior margin. This orientation brings the CS musculature to a close relation beneath the compact AV node. In Group B (superficial extension, *Figure 4B*), another tricuspid valve anatomical pattern is shown in which the tricuspid valve is straight, pushing the CS opening more posteriorly. In this group, the CS opening is facing the compact AV node by its antero-superior margin, an orientation that brings the CS musculature away from the level of the compact AV node. There was no significant difference between both groups regarding age, sex, heart weight, CS diameter, and the septal isthmus length (*Table 2*).

Discussion

The AV conduction axis begins from the top of the Koch's triangle.[1] It then penetrates the central fibrous body, and bifurcates into bundle branches beneath the membranous septum. The histological approach for the AV node has not been changed since Tawara's monograph was established.[8] In that method, the histological exploration of the AV conduction axis has mainly been

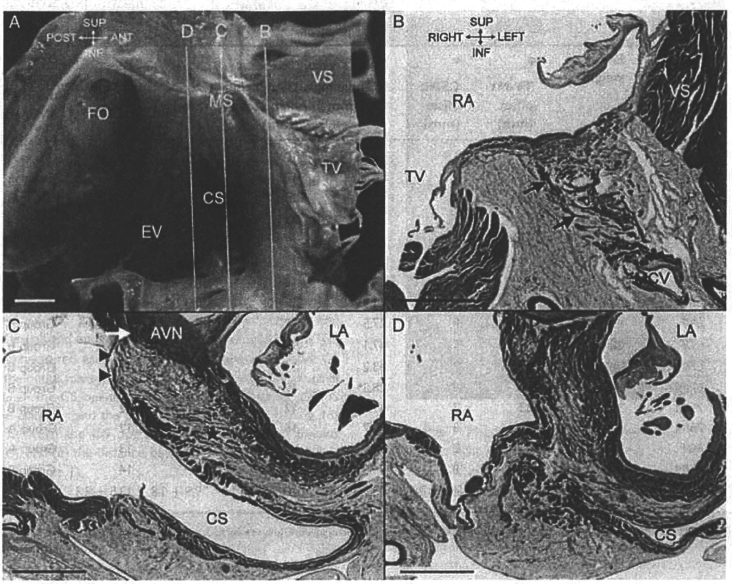

Figure 2 Representative of hearts with the Group A (the coronary sinus musculature deeply extends into the atrioventricular septum). (*A*) The macroscopic endocardial view of the Koch's triangle. Three lines (*B–D*) show the levels of histological sections. (*B*) Level B is within the septal isthmus, the coronary sinus musculature intrudes into the atrioventricular septal junction and merges with vestibule myocardium (black arrows). (*C*) Level C is through the middle part of the coronary sinus opening, the coronary sinus musculature shows loose connections with the left atrial myocardium (black star) just behind the atrioventricular node. The black arrow heads show the thin strand of transitional cells which are interposing between the atrioventricular node and the intermingled muscles of coronary sinus and vestibule. The white arrow shows the junction of the atrioventricular node and the penetrating bundle of His. (*D*) Level D is the posterior margin of the coronary sinus opening adjacent to the Eustachian ridge, the coronary sinus musculature scarcely has connections with left and right atrial myocardium. The connection between both atria through the coronary sinus musculature is observed mainly at the anterior border of the coronary sinus opening (No. 2, 26-year-old male). ANT, anterior; AVN, atrioventricular node; CS, coronary sinus; EV, Eustachian valve; FO, foramen ovale; INF, inferior; LA, left atrium; MCV, middle cardiac vein; MS, membranous septum; MV, mitral valve; POST, posterior; RA, right atrium; SUP, superior; TV, tricuspid valve; VS, ventricular septum. Bars = 5 mm.

performed by vertically sliced sections of the AV annuli, and this method has been applied for many years.[9] The CS opening is one of the elements composing the Koch's triangle.[1] However, these traditional vertically sliced sections of the Koch's triangle had technical limitations with regard to observing the histological structure of the lower part of the Koch's triangle, including CS opening due to its curvature and the divergence of both mitral and tricuspid annuli. Our histological method employed in this study, in which we made sections parallel to both annuli, provides the reference to the relation between the dimensions of Koch's triangle and the arrangement of CS musculature. Furthermore, these specimens showed both atria in the famous clinical fluoroscopical left anterior oblique (LAO) view style and made it easy to observe myocardial connections between both atria. Chauvin *et al.*[5] described the myocardial connections between the left atrial myocardium and the CS musculature using a similar method. Furthermore, Racker and Kadish[10] highlighted the myocardial arrangement within the AV node using the three-plane histological sectioning in dog hearts. However, they have not explored the myocardial arrangement around the AV septal junction. Inoue and Becker[11] described the distribution of the compact node and its extensions with reference to the substrate of the slow pathway in AVNRT in the AV septal junction. In their study, however, spatial distribution of the CS musculature around the AV nodal tissue was not mentioned. The present study with short-axis style sections unveiled the right and left atrial connection beneath the septal isthmus. This myocardial area that might participate in AVNRT was shown in a single autopsy case report.[12]

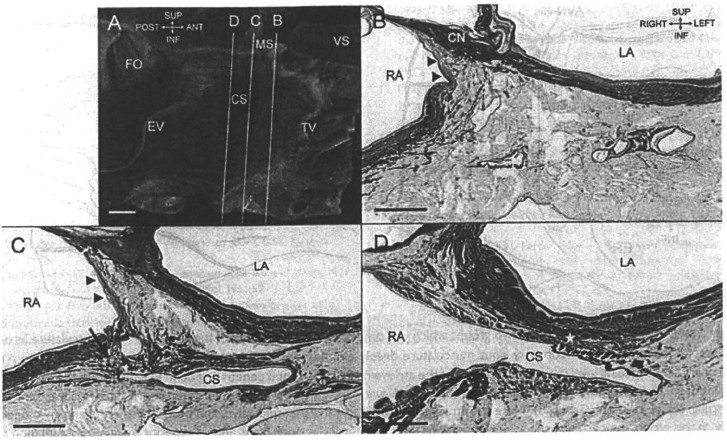

Figure 3 Representative of the hearts with Group B (the coronary sinus musculature superficially extends above the atrioventricular septal junction). (*A*) The macroscopic endocardial view of Koch's triangle. Three lines (*B–D*) show the levels of histological sections. (*B*) Level B is within the septal isthmus, myocardial connection between the both atria is hardly observed except for the compact atrioventricular node. The black arrow heads show the indirect continuity between the atrioventricular node and the vestibule muscle of the right atrium. This thin muscle strand shows the transitional cells. (*C*) Level C is the anterior part of the coronary sinus opening, the coronary sinus musculature merges within the right atrial myocardium at the antero-superior border of coronary sinus opening. The black arrow heads show the transitional cells. (*D*) Level D is through the posterior margin of coronary sinus opening, the coronary sinus musculature adheres to the left atrial myocardium (white star). (No. 9, 66-year-old female). ANT, anterior; CS, coronary sinus; CN, compact node; ER, Eustachian ridge; FO, foramen ovale; INF, inferior; LA, left atrium; MS, membranous septum; MV, mitral valve; POST, posterior; RA, right atrium; SUP, superior; TV; tricuspid valve; VS, ventricular septum. Bars = 5 mm.

Table 2 Comparison between the two groups

Distribution pattern of CS musculature into AV septum		Group A ($n = 8$)	Group B ($n = 8$)	*P*-value
Age (years)		51.3 ± 20.4	64.6 ± 13.9	n.s ($P = 0.15$)
Heart weight (g)		309.3 ± 85.9	360.6 ± 58.3	n.s. ($P = 0.18$)
a	TV-MV offset (mm)	3.8 ± 1.4	2.4 ± 1.1	$P = 0.04$
b	CS-MS offset (mm)	2.8 ± 1.9	5.8 ± 2.9	$P = 0.03$
c	CS opening size (mm^2)	48.3 ± 23.0	39.1 ± 7.8	n.s. ($P = 0.30$)
	CS-diameter (mm)	11.0 ± 2.9	10.0 ± 2.8	n.s. ($P = 0.49$)
d	CS-TV dimension (mm)	9.5 ± 1.8	10.3 ± 1.8	n.s. ($P = 0.42$)
e	CS-MS dimension (mm)	14.8 ± 1.6	12.3 ± 2.2	$P = 0.02$

AV, atrioventricular; CS, coronary sinus; MS, membranous septum; MV, mitral valve; TV, tricuspid valve; a-e, see *Figure 1*.

The concern about the exploration of the CS morphology, dilatation of the CS opening, or increase of the CS volume was reported using CS angiography or intracardiac ultrasounds in AVNRT cases.[13,14] Furthermore, DeLurgio *et al.*[15] have also reported a good correlation between CS volume and the presence of dual AV nodal physiology in case of AVNRT. For this reason, it is supposed that small morphological variations of the CS may provide some substrates of AVNRT. We could not calculate the real volume of the AV septal junction in these specimens, though the CS opening-membranous septum dimension was longer in CS deep extension group (Group A) than in the superficial extension group (Group B). We have reached the conclusion that not

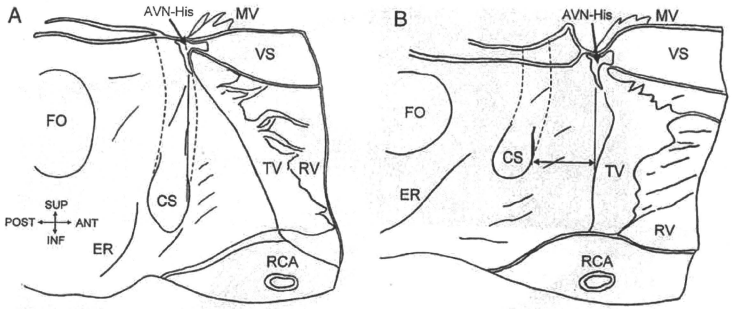

Figure 4 The schematic representation of two groups which was divided by the distribution of the coronary sinus musculature into the atrioventricular septal junction. (*A*) The coronary sinus musculature deeply extends into the atrioventricular septal junction (Group A). In these hearts, coronary sinus opening level is close to the level of the atrioventricular node and penetrating bundle of His. Note the normal downward displacement of tricuspid valve annulus into the right ventricle in *Figure 2A*. (*B*) The coronary sinus musculature superficially extends above the atrioventricular septal junction (Group B). Note the straight attachment of the tricuspid valve, and pushing the coronary sinus opening more posteriorly. In this group, the coronary sinus opening is facing the atrioventricular node by its antero-superior margin, an orientation that brings the coronary sinus musculature away from the level of the atrioventricular node. ANT, anterior; AVN, atrioventricular node; CS, coronary sinus; ER, Eustachian ridge; FO, foramen ovale; INF, inferior; LA, left atrium; MV, mitral valve; POST, posterior; RA, right atrium; RCA, right coronary artery; RV, right ventricle; SUP, superior; TV, tricuspid valve; VS, ventricular septum.

only AV nodal anatomy, but also the spatial distributions of the CS musculature, may have a role in the pathology of AVNRT, and both of them should be investigated in AVNRT cases. Furthermore, the characteristics provided by CS morphology may be of more significance in the left variant AVNRT cases, because in these cases, the ablation therapy is sometimes performed within the CS.[16]

Ho *et al.*[4] mentioned the myocardial arrangement around the compact AV node in patients with electrophysiologically proven dual AV nodal pathway using the conventional vertical histological sections. They focused on the distribution of transitional fibres approaching the AV node and found three patterns (superficial, deep, and posterior), but they concluded that the substrate of multiple pathways was ubiquitous. In our study, using the histological LAO view, both of the left and right atrial vestibules had connections with the CS musculature. In addition, the myocardial arrangements, including the CS musculature within the AV septal junction, showed non-uniformity and this phenomenon seems to be related to some of the electrical characteristics in this area.

Limitations

Because of the uncertainty in the cell-to-cell coupling under the optical microscope using the conventional staining of our study, quantification of the myocardial connections between CS musculature and the proximal AV conduction axis or the left and right atrial myocardium was not possible. We consider that using immunohistochemical staining methods, such as gap junction protein, might add information in this concern.

Although short-axis sections facilitate the histological observation of myocardial arrangements within the AV septal junction, myocardial arrangements do not always coincide with the electrophysiological phenomena. Recent experimental simulation showed that the transitional cells around the AV node and nodal extensions are associated with the formations of reentrant circuits.[17] Concerning about the participation of the CS musculature in AVNRT cases, accumulation of autopsy findings after successful ablation procedure should be required.

Conclusion

The CS location provides the variations of the muscular arrangements within the AV septal junction. Especially, the deep extension of the CS musculature into the AV septal junction seems to increase the tissue non-uniformity around the AV node.

Acknowledgements

The authors thank Ms Yoshiko Sasaki (Second Department of Pathology, Showa University School of Medicine, Tokyo) and Mr Nobuyoshi Imai (Department of Pathology, National Cardiovascular Center) for their technical support and also thank Dr Alaa Mabrouk Omar MSc. (Assistant Researcher of Cardiology, NRC, Cairo, Egypt) for his kind English language support.

Conflict of interest: none declared.

References

1. Koch W. Weiter mitteilungen uber den Sinusknoten der Herzens Verh. *Deutsh Path Gesell* 1909;**13**:85–98.
2. Inoue S, Becker AE. Koch's triangle sized up: anatomical landmarks in perspective of catheter ablation procedures. *Pacing Clin Electrophysiol* 1998;**21**:1553–8.

3. Jackman WM, Beckman KJ, McClelland JH, Wang X, Friday KJ, Roman CA *et al.* Treatment of supraventricular tachycardia due to antrioventricular nodal reentry, by radiofrequency catheter ablation of slow-pathway conduction. *N Engl J Med* 1992;**327**:313–8.
4. Ho SY, McComb JM, Scott CD, Anderson RH. Morphology of the cardiac conduction system in patients with electrophysiologically proven dual atrioventricular nodal pathway. *J Cardiovasc Electrophysiol* 1993;**4**:504–12.
5. Chauvin M, Shah DC, Haïssaguerre M, Marcellin L, Brechenmacher C. The anatomic basis of connections between the coronary sinus musculature and the left atrium in humans. *Circulation* 2000;**101**:647–52.
6. Lüdinghausen M, Ohmachi M, Boot C. Myocardial coverage of the coronary sinus and related veins. *Clin Anat* 1992;**5**:1–15.
7. Cabrera JA, Sanchez-Quintana D, Ho SY, Medina A, Anderson RH. The architecture of the atrial musculature between the orifice of the inferior caval vein and the tricuspid valve: the anatomy of the isthmus. *J Cardiovasc Electrophysiol* 1998;**9**:1186–95.
8. Tawara S. *Das Reizleitungssystem des Säugetierherzens. Eine anatomisch-histologische studie über das atrioventrikularbündel und die Purkinjeschen fäden.* Jena, Germany: Gustav Fischer; 1906.
9. Lev M, Widran J, Erickson EE. A method for the histopathologic study of the atrioventricular node, bundle, and branches. *AMA Arch Pathol* 1951;**52**:73–83.
10. Racker DK, Kadish AH. Proximal atrioventricular bundle, atrioventricular node, and distal atrioventricular bundle are distinct anatomic structures with unique histological characteristics and innervation. *Circulation* 2000;**101**:1049–59.
11. Inoue S, Becker AE. Posterior extensions of the human compact atrioventricular node. A neglected anatomic feature of potential clinical significance. *Circulation* 1998;**97**:188–93.
12. Inoue S, Becker AE, Riccardi R, Gaita F. Interruption of the inferior extension of the compact atrioventricular node underlies successful radio frequency ablation of atrioventricular nodal reentrant tachycardia. *J Interv Card Electrophysiol* 1999; **3**:273–7.
13. Doig JC, Saito J, Harris L, Downar E. Coronary sinus morphology in patients with atrioventricular junctional reentry tachycardia and other supraventricular tachyarrhythmias. *Circulation* 1995;**92**:436–41.
14. Okumura Y, Watanabe I, Yamada T, Ohkubo K, Masaki R, Sugimura H *et al.* Comparison of coronary sinus morphology in patients with and without atrioventricular nodal reentrant tachycardia by intracardiac echocardiography. *J Cardiovasc Electrophysiol* 2004;**15**:269–73.
15. DeLurgio DB, Frohwein SC, Walter PF, Langberg JJ. Anatomy of atrioventricular nodal reentry investigated by intracardiac echocardiography. *Am J Cardiol* 1997;**80**: 231–3.
16. Otomo K, Okamura H, Noda T, Satomi K, Shimizu W, Suyama K *et al.* 'Left-variant' atypical atrioventricular nodal reentrant tachycardia: electrophysiological characteristics and effect of slow pathway ablation within coronary sinus. *J Cardiovasc Electrophysiol* 2006;**17**:1177–83.
17. Li J, Greener ID, Inada S, Nikolski VP, Yamamoto M, Hancox JC *et al.* Computer three-dimensional reconstruction of the atrioventricular node. *Circ Res* 2008;**102**: 975–85.

High prevalence of early repolarization in short QT syndrome

Hiroshi Watanabe, MD, PhD, FESC,* Takeru Makiyama, MD, PhD,† Taku Koyama, MD,‡ Prince J. Kannankeril, MD, MSCI,¶ Shinji Seto, MD,§ Kazuki Okamura, MD, PhD,‖ Hirotaka Oda, MD, PhD,‖ Hideki Itoh, MD, PhD,** Masahiko Okada, MD, PhD,†† Naohito Tanabe, MD, PhD,‡‡ Nobue Yagihara, MD,* Shiro Kamakura, MD, PhD,† Minoru Horie, MD, PhD,** Yoshifusa Aizawa, MD, PhD,* Wataru Shimizu, MD, PhD‡

*From the *Division of Cardiology, Niigata University Graduate School of Medical and Dental Sciences, Niigata, Japan, †Department of Cardiovascular Medicine, Kyoto University Graduate School of Medicine, Kyoto, Japan, ‡Division of Cardiology, Department of Internal Medicine, National Cardiovascular Center, Suita, Japan, ¶Department of Pediatrics, Vanderbilt University School of Medicine, Nashville, Tennessee, §Department of Cardiology, Inoue Hospital, Nagasaki, Japan, ‖Department of Cardiology, Niigata City General Hospital, Niigata, Japan, **Department of Cardiovascular and Respiratory Medicine, Shiga University of Medical Science, Shiga, Japan, ††Department of Laboratory Medicine, Niigata University Graduate School of Medical and Dental Sciences, Niigata, Japan, and ‡‡Division of Health Promotion, Niigata University Graduate School of Medical and Dental Sciences, Niigata, Japan.*

BACKGROUND Short QT syndrome (SQTS) is characterized by an abnormally short QT interval and sudden death. Due to the limited number of cases, the characteristics of SQTS are not well understood. It has been reported recently that early repolarization is associated with idiopathic ventricular fibrillation and the QT interval is short in patients with early repolarization.

OBJECTIVE The purpose of this study was to study the association between early repolarization and arrhythmic events in SQTS.

METHODS The study consisted of three cohorts: SQTS cohort (N = 37), control cohort with short QT interval and no arrhythmic events (N = 44), and control cohort with normal QT interval (N = 185). ECG parameters were compared among the study cohorts.

RESULTS Heart rate, PR interval, and QRS duration were similar among the three study cohorts. Early repolarization was more common in the SQTS cohort (65%) than in the short QT control cohort (30%) and the normal QT control cohort (10%). Duration from T-wave peak to T-wave end was longer in the SQTS cohort than in the short QT control cohort, although QT and corrected QT intervals were similar. In the SQTS cohort, there were more males among patients with arrhythmic events than in those with a family history but without arrhythmic events. In multivariate models, early repolarization was associated with arrhythmic events in the SQTS cohort. ECG parameters including QT and QTc intervals were not associated with arrhythmic events in the SQTS cohort.

CONCLUSION There is a high prevalence of early repolarization in patients with SQTS. Early repolarization may be useful in identifying risk of cardiac events in SQTS.

KEYWORDS Arrhythmia; Electrocardiogram; QT interval; Repolarization; Sudden death

ABBREVIATIONS **QTc** = corrected QT interval; **SQTS** = short QT syndrome

(Heart Rhythm 2010;7:647–652) © 2010 Heart Rhythm Society. All rights reserved.

Introduction

The short QT syndrome (SQTS) is characterized by an abnormally short QT interval and increased risk of ventricular fibrillation and sudden death.[1,2] Similar to other arrhythmia syndromes, such as long QT syndrome and Brugada syndrome,[3] SQTS is a genetically heterogeneous disease, and, to date, five responsible genes encoding different ion channels have been identified.[3–7] Some inherited arrhythmia syndromes may share genetic backgrounds that result in overlapping arrhythmia phenotypes.[3]

Although early repolarization is generally considered benign,[8] it has been reported recently that early repolarization is associated with increased risk for sudden cardiac death in patients with idiopathic ventricular fibrillation.[9–12] Haissaguerre et al[9] reported that, among patients with idiopathic ventricular fibrillation, the QT interval was shorter in patients with early repolarization than in those without, suggesting an association between early repolarization and QT interval shortening. Evidence that mutations in calcium channel genes are associated with Brugada-type ST-segment elevation and abnormally short QT intervals further suggests a relationship between early phase repolarization abnormalities and short QT interval.[4] Here we report on our

Drs. T. Makiyama, M. Horie, and W. Shimizu were supported in part by the Research Grant for the Cardiovascular Diseases (21C-8) from the Ministry of Health, Labour and Welfare, Japan. **Address reprint requests and correspondence:** Dr. Wataru Shimizu, Division of Cardiology, Department of Internal Medicine, National Cardiovascular Center, 5-7-1 Fujishiro-dai, Suita 565-8565, Japan. E-mail address: wshimizu@hsp.ncvc.go.jp. (Received November 29, 2009; accepted January 9, 2010.)

study of the prevalence of early repolarization and its association with arrhythmic events in SQTS.

Methods

This cooperative study consisted of three cohorts. (1) *SQTS cohort* included patients with SQTS referred to our institutions and patients with SQTS from previous reports. The diagnosis of SQTS was made if a patient with a short QT interval [corrected QT interval (QTc) by Bazett formula ≤330 ms] had an arrhythmic event including documented ventricular fibrillation, resuscitated sudden cardiac death, and syncope and/or had a family history of SQTS, or if a patient with a short QT interval (QTc ≤360 ms) had mutations in ion channel genes responsible for SQTS.[3,13] We searched in the electronic databases PubMed, EMBASE, and Cochrane for all published studies that examined patients with SQTS. The search was limited to the end of June 2009. Published studies were considered eligible if they included clinical characteristics of the patients and ECGs. All ECGs from patients reported in the literature were reanalyzed. Electrophysiologic study was performed in patients with SQTS based on the indication of each institution. (2) *Control cohort with short QT interval* (QTc ≤330 ms) *and no arrhythmic events* was selected from among 86,068 consecutive ECGs stored on the ECG database at Niigata University Medical and Dental Hospital from May 7, 2003 to July 2, 2009. Subjects who did not have arrhythmic events or cardiovascular disease and were not taking any medication were included in this cohort. (3) *Control cohort with normal QT interval* was also selected from the ECG database. This cohort consisted of subjects who were matched to the SQTS cohort for gender and age. Subjects who had normal QT interval (360–440 ms) and did not have cardiovascular disease or were not taking any medication were included in this cohort. Subjects with Brugada-type ST-segment elevation were excluded from all study cohorts.[3,9]

QT intervals were measured on lead V_2 with the tangent methods for determination of QT_{end} using a semi-automated digitizing program with electronic calipers by an experienced observer blinded to the clinical details of all subjects included in this study.[14,15] Early repolarization was defined as elevation of the J point noted as either as QRS slurring or notching ≥0.1 mV in more than two leads.[9]

Differences in parameters were analyzed using multivariable logistic regression models when SQTS cohort and control cohort with short QT interval were compared and analyzed using conditional logistic regression models when SQTS cohort and control cohort with normal QT interval were compared. All statistical analyses were performed with SPSS (version 12.0, SPSS, Inc., Chicago, IL, USA). Two-sided $P < .05$ was considered significant. Values are expressed as mean ± SD. The study protocol was approved by the Ethics Committee of Niigata University School of Medicine. To determine interobserver variability, a second observer made independent blinded QT interval determinations of all study subjects with short QT interval.

Results

Thirty-seven patients with SQTS were identified: 12 from our institutions and 25 reported in the literature,[2,5,6,14,16–25] Forty-four control subjects with short QT interval and 185 control subjects with normal QT interval also were identified (Table 1). The SQTS cohort consisted of 25 (68%) patients with symptoms, including 14 with cardiac arrest (3 sudden death, 11 resuscitated) and 11 with syncope. Genetic screening identified mutations in ion channels in 7 (41%) of 17 probands who were genetically screened (2 *KCNQ1*, 4 *KCNH2*, 1 *KCNJ2*). Among patients in our institutions and those reported in the literature, there was no difference with regard to gender, age, prevalence of family history, QT or QTc interval, or inducibility of ventricular tachyarrhythmia by electrical programmed stimulation.

Heart rate, PR interval, and QRS duration in the SQTS cohort were not different among patients in either the short QT control cohort or the normal QT control cohort (Table 1). QT and corrected QT intervals were shorter in the SQTS and short QT control cohorts than in the normal QT control cohort. Early repolarization occurred in 24 (65%) patients with SQTS (Figure 1). Interobserver variability between two investigators was 8.6 ms (95% confidence interval −0.5 to 17.7 ms) for QT interval and 9.0

Table 1 ECG parameters of study cohorts

	Patients with SQTS (N = 37)	Subjects with short QTc (N = 44)	Versus subjects with short QTc*		Subjects with normal QTc† (N = 185)	Versus subjects with normal QTc	
			OR (95% CI)	*P* value		OR (95% CI)	*P* value
Male gender [N (%)]	27 (73)	34 (77)	2.84 (0.72–11.2)	.14	135 (73)	—	—
Age (years)	30 ± 19	47 ± 23	1.05 (1.02–1.08)	.001	30 ± 19	—	—
Heart rate (bpm)	69 ± 393	65 ± 398	1.00 (1.00–1.01)	.3	70 ± 327	1.00 (1.00–1.00)	0.70
PR interval (ms)	138 ± 19	153 ± 38	1.01 (0.99–1.03)	.54	143 ± 24	0.99 (0.97–1.01)	0.18
QRS interval (ms)	86 ± 7	84 ± 8	0.97 (0.91–1.04)	.38	85 ± 7	1.01 (0.96–1.06)	0.74
QT interval (ms)	286 ± 36	286 ± 15	0.99 (0.97–1.01)	.28	367 ± 36	0.97 (0.96–0.98)	<0.001
QTc (ms)	308 ± 29	299 ± 21	0.98 (0.96–1.00)	.06	399 ± 24	0.97 (0.97–0.98)	<0.001

CI = confidence interval; OR = odds ratio; QTc = corrected QT interval; SQTS = short QT syndrome.

*Models were adjusted for gender and age.

†Gender and age were matched between patients with SQTS and subjects with normal QT interval.

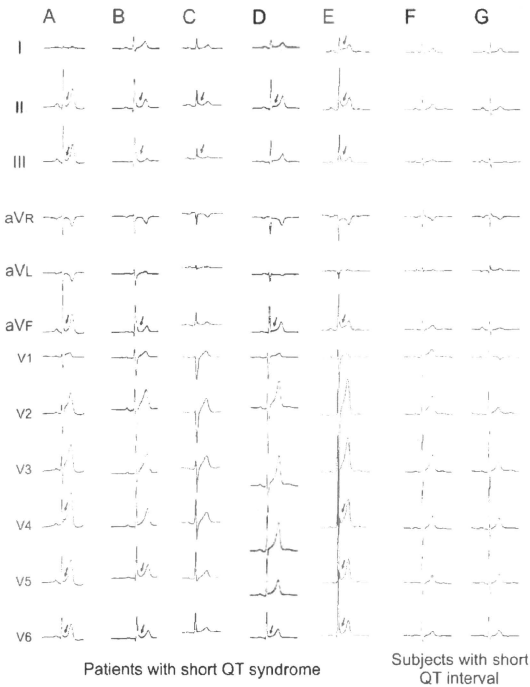

Figure 1 Early repolarization in short QT syndrome. ECGs were recorded from patients with short QT syndrome (**A:** 61-year-old woman; **B:** 30-year-old man; **C:** 38-year-old man; **D:** 31-year-old man; **E:** 22-year-old man) and control subjects with a short QT interval (**F:** 23-year-old man; **G:** 44-year-old woman). In each patient with short QT syndrome, early repolarization was evident in the inferolateral leads (*arrows*).

ms (95% confidence interval −0.6 to 18.7 ms) for QTc interval. The frequency of early repolarization was not different between patients in our institutions and those reported in the literature. Early repolarization was present in the inferior leads (II, III, aVF) in 9 patients, in the lateral leads (I, aVL, V_4–V_6) in 6 patients, and in both the inferior and lateral leads in 9 patients. Of 10 probands with early repolarization genetically screened, mutations were identified in 3 patients (1 *KCNQ1*, 2 *KCNH2*). Early repolarization was more common in the SQTS cohort than in the short QT control and normal QT control cohorts (Figure 2).

The association of early repolarization with arrhythmic events then was studied in patients with SQTS. In the SQTS cohort, there were more males among patients with arrhythmic events than among those with a family history but without arrhythmic events (Table 2). In multivariate models adjusted for gender and age, early repolarization was associated with arrhythmic events, although ECG parameters including QT and QTc intervals were not associated with arrhythmic events. Early repolarization remained associated with arrhythmic events after adjustment for age, gender, and QTc interval (P = .001). Electrophysiologic study performed in 18 patients with SQTS revealed no difference in inducibility of ventricular tachyarrhythmia between patients with arrhythmic events (73%) and those without arrhythmic events (71%).

QT interval parameters were compared between SQTS and short QT control cohorts because some of the parameters recently have been associated with SQTS.[26] Interval from T-wave peak to T-wave end (T_{peak} to T_{end}) was longer in the SQTS cohort than in the short QT control cohort even after heart rate correction using the Bazett formula, whereas QT interval, QTc interval, and interval from Q-wave to T-wave peak (QT_{peak}) were not different between the two cohorts (Table 3). Ratio of T_{peak} to T_{end} per QT was larger in the SQTS cohort than in the short QT control cohort.

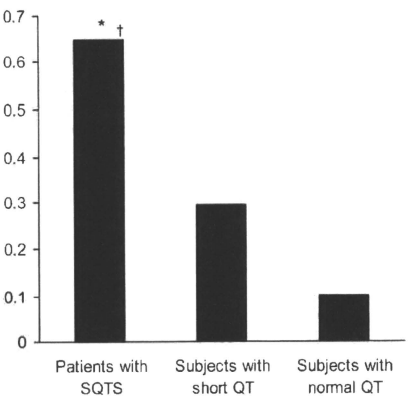

Figure 2 Frequency of early repolarization. Odds ratios (95% confidence intervals) for early repolarization in patients with short QT syndrome (SQTS) were 5.64 (1.97–16.15) and 16.58 (7.2–38.21) versus subjects with short QT interval and those with normal QT interval, respectively. *P = .001 vs subjects with short QT interval. †P <.001 vs subjects with normal QT interval.

Discussion

SQTS is a recently discovered, very rare disease with an increased risk of sudden death.[2] Due to the limited number of cases, the characteristics of SQTS are not well understood. Therefore, we conducted a cooperative analysis of ECGs from patients with SQTS in our institutions and those reported in the literature and found that early repolarization is common in SQTS.

Early repolarization is a common ECG finding. It is present in 1% to 13% of the general population and usually is considered as a normal variant due to its benign long-term prognosis.[8,11,27–29] However, increasing evidence suggests that early repolarization is associated with arrhythmia.[9,27,30–34] Since 1985, we and other investigators have reported an association between early repolarization (or late depolarization) and sudden cardiac death.[30–32] A multicenter study including our institution recently showed that early repolarization is present in one third of patients with idiopathic ventricular fibrillation.[9] Early repolarization is associated with increased risk of sudden cardiac arrest in idiopathic ventricular fibrillation, and the amplitude of early repolarization increases before development of arrhythmic events.[9,10] In Brugada syndrome, which is characterized by J-wave and ST-segment elevation in the right precordial leads on ECG and sudden cardiac death,[3] early repolarization in the inferolateral leads is not uncommon and is associated with arrhythmic events,[34] although another report has shown negative results.[33] In our study, early repolarization in the inferolateral leads was frequently found in SQTS and, more importantly, was associated with arrhythmic events in SQTS. In addition to arrhythmia syndromes unassociated with structural heart disease, a high frequency of early repolarization in arrhythmogenic right ventricular dysplasia/cardiomyopathy has been reported.[27]

It has been suggested that SQTS and idiopathic ventricular fibrillation share clinical characteristics.[23] Short QT interval is frequently found in idiopathic ventricular fibrillation,[23] and QT interval is relatively short in patients with idiopathic ventricular fibrillation who have early repolarization.[9] Spontaneous and inducible ventricular fibrillation can be initiated by short-coupled premature ventricular beat in SQTS and idiopathic ventricular fibrillation.[21,35,36] The efficacy of isoproterenol and quinidine has been reported for both arrhythmia syndromes,[21,37] although the arrhythmogenic effects of isoproterenol in an experimental model of SQTS have been reported.[38] Our study showing an association of early repolarization with SQTS further supports the presence of common arrhythmogenic substrates in SQTS and idiopathic ventricular fibrillation.

A precise mechanism for ventricular fibrillation in SQTS is not known, but characteristic ECG abnormalities may reflect arrhythmogenicity. A prior study showed that the interval from T-wave peak to T-wave end is relatively long in SQTS, and our study replicated the results.[26] T-wave peak to T-wave end interval is considered to reflect transmural dispersion of repolarization, and relative prolongation of the interval in SQTS may indicate a high vulnerability to ventricular fibrillation.[39] An experimental model of SQTS

Table 2 Characteristics of SQTS patients with and those without arrhythmic events

	Patients with arrhythmic events (N = 25)	Patients without arrhythmic events (N = 12)	OR (95% CI)	*P* value
Male gender [N (%)]	21 (84)	6 (50)	10.44 (0.85–127.48)	.07
Age (years)	30 ± 19	23 ± 18	1.05 (0.99–1.12)	.13
Heart rate (bpm)	69 ± 393	76 ± 473	1.00 (1.00–1.01)	.38
PR interval (ms)	138 ± 19	134 ± 18	0.99 (0.95–1.04)	.84
QRS interval (ms)	86 ± 7	85 ± 10	0.93 (0.82–1.07)	.31
QT interval (ms)	286 ± 36	271 ± 40	1.00 (0.97–1.03)	.75
QTc (ms)	308 ± 29	306 ± 33	0.98 (0.94–1.02)	.33
Early repolarization [N (%)]	22 (88)	2 (17)	46.53 (4.52–478.79)	.001

CI = confidence interval; OR = odds ratio; QTc = corrected QT interval; SQTS = short QT syndrome.
Models were adjusted for gender and age.

Table 3 ECG parameters for study cohorts with short QT interval

	Patients with SQTS	Subjects with short QTc	OR (95% CI)	*P* value
QT_{peak} (ms)	211 ± 37	222 ± 19	0.99 (0.98–1.01)	.37
Corrected QT_{peak}	226 ± 32	234 ± 24	0.99 (0.98–1.01)	.56
T_{peak} to T_{end} (ms)	81 ± 21	67 ± 13	1.08 (1.03–1.13)	<.001
Corrected T_{peak} to T_{end}	89 ± 28	72 ± 17	1.05 (1.02–1.09)	.002
QT_{peak}/QT ratio (%)	27 ± 6	22 ± 4	0.83 (0.73–0.94)	.004

Models were adjusted for gender and age.
CI = confidence interval; OR = odds ratio; QTc = corrected QT interval; SQTS = short QT syndrome.

provides evidence that increased transmural dispersion of repolarization under short QT interval conditions results in ventricular tachyarrhythmia.[38] A tall peaked T wave is one of the characteristic ECG abnormalities in SQTS,[1] but the amplitude of the T wave is not different between patients with SQTS and subjects with short QT interval and no arrhythmic events, suggesting that a tall T wave is associated with a short QT interval but is not associated with arrhythmogenicity.[26] In SQTS, characteristic ECG abnormities are also found in the early repolarization phase. In patients with SQTS, the ECG shows a very short J-point to T-wave peak interval and no flat ST segment.[26] In our study, early repolarization was frequently found in SQTS and was associated with arrhythmic events. Whether the inferolateral J-point elevation reflects late depolarization or early repolarization is controversial, but this pattern has been considered repolarization because of slower inscription, spontaneous changes occurring concurrently with ST segment but not with QRS complexes, and absence of late potentials on signal-averaged ECG.[9,40] Taken together, the finding suggest that abnormalities in the early phase of repolarization create the arrhythmogenic substrate in SQTS.

Sex hormone and gender difference have an important role in the arrhythmia syndromes.[41–43] It is well known that the QT interval is affected by sex hormones, and the QT interval is longer in women than men.[44] Female gender is a risk factor for development of ventricular tachyarrhythmias in both congenital and acquired long QT syndrome.[41,42] On the other hand, Brugada syndrome is more prevalent in men than in women, and the male hormone testosterone is reported to contribute to male predominance in Brugada syndrome.[43] In this study, male gender was associated with arrhythmic events in SQTS and short QT interval was frequently found in men, suggesting a role of sex hormones in SQTS opposite to that in long QT syndrome. Recent evidence that the QT interval can be shortened by anabolic androgenic steroids and testosterone further supports this hypothesis.[45,46]

SQTS is a genetically heterogeneous disease with five responsible genes encoding ion channels: *KCNQ1*, *KCNH2*, *KCNJ2*, *CACNA2D1*, and *CACNB2b*.[3,4] An increase in outward current by gain-of-function mutations in potassium channels or a decrease in inward current by loss of function mutations in calcium channels may be responsible for SQTS.[3,4] Early repolarization was found in patients with mutations in *KCNQ1* and *KCNH2* and in those without mutations in the known genes, suggesting a heterogeneous genetic background for the association between short QT interval and early repolarization. To date, mutations in calcium channel genes (*CACNA2D1* and *CACNB2b*) have been identified in three probands with Brugada syndrome associated with a short QT interval, but early repolarization is not present in the inferolateral leads in any of them.[4] A recent study has identified a mutation in *KCNJ8*, an initial responsible gene for idiopathic ventricular fibrillation associated with early repolarization.[47] Although there are some similarities in phenotype between SQTS and idiopathic ventricular fibrillation with early repolarization, a common genetic background has not been identified.

Conclusion

Our study showed a high prevalence of early repolarization in patients with SQTS and an association of early repolarization with arrhythmic events. Early repolarization may be a useful marker for risk stratification of cardiac arrest in SQTS, although further investigation with longitudinal follow-up is required to evaluate our results.

References

1. Gussak I, Brugada P, Brugada J, et al. Idiopathic short QT interval: a new clinical syndrome? Cardiology 2000;94:99–102.
2. Gaita F, Giustetto C, Bianchi F, et al. Short QT syndrome: a familial cause of sudden death. Circulation 2003;108:965–970.
3. Lehnart SE, Ackerman MJ, Benson DW Jr, et al. Inherited arrhythmias: a National Heart, Lung, and Blood Institute and Office of Rare Diseases workshop consensus report about the diagnosis, phenotyping, molecular mechanisms, and therapeutic approaches for primary cardiomyopathies of gene mutations affecting ion channel function. Circulation 2007;116:2325–2345.
4. Antzelevitch C, Pollevick GD, Cordeiro JM, et al. Loss-of-function mutations in the cardiac calcium channel underlie a new clinical entity characterized by ST-segment elevation, short QT intervals, and sudden cardiac death. Circulation 2007;115:442–449.
5. Brugada R, Hong K, Dumaine R, et al. Sudden death associated with short-QT syndrome linked to mutations in HERG. Circulation 2004;109:30–35.
6. Bellocq C, van Ginneken AC, Bezzina CR, et al. Mutation in the KCNQ1 gene leading to the short QT-interval syndrome. Circulation 2004;109:2394–2397.
7. Priori SG, Pandit SV, Rivolta I, et al. A novel form of short QT syndrome (SQT3) is caused by a mutation in the KCNJ2 gene. Circ Res 2005;96:800–807.
8. Klatsky AL, Oehm R, Cooper RA, et al. The early repolarization normal variant electrocardiogram: correlates and consequences. Am J Med 2003;115:171–177.
9. Haissaguerre M, Derval N, Sacher F, et al. Sudden cardiac arrest associated with early repolarization. N Engl J Med 2008;358:2016–2023.
10. Nam GB, Kim YH, Antzelevitch C. Augmentation of J waves and electrical storms in patients with early repolarization. N Engl J Med 2008;358:2078–2079.
11. Rosso R, Kogan E, Belhassen B, et al. J-point elevation in survivors of primary ventricular fibrillation and matched control subjects: incidence and clinical significance. J Am Coll Cardiol 2008;52:1231–1238.
12. Viskin S. Idiopathic ventricular fibrillation "Le Syndrome d'Haissaguerre" and the fear of J waves. J Am Coll Cardiol 2009;53:620–622.

13. Viskin S. The QT interval: too long, too short or just right. Heart Rhythm 2009;6:711–715.
14. Extramiana F, Maury P, Maison-Blanche P, et al. Electrocardiographic biomarkers of ventricular repolarisation in a single family of short QT syndrome and the role of the Bazett correction formula. Am J Cardiol 2008;101:855–860.
15. Watanabe H, Kaiser DW, Makino S, et al. ACE I/D polymorphism associated with abnormal atrial and atrioventricular conduction in lone atrial fibrillation and structural heart disease: implications for electrical remodeling. Heart Rhythm 2009;6:1327–1332.
16. Anttonen O, Vaananen H, Junttila J, et al. Electrocardiographic transmural dispersion of repolarization in patients with inherited short QT syndrome. Ann Noninvas Electrocardiol 2008;13:295–300.
17. Giustetto C, Di Monte F, Wolpert C, et al. Short QT syndrome: clinical findings and diagnostic-therapeutic implications. Eur Heart J 2006;27:2440–2447.
18. Hong K, Bjerregaard P, Gussak I, et al. Short QT syndrome and atrial fibrillation caused by mutation in KCNH2. J Cardiovasc Electrophysiol 2005;16:394–396.
19. Kirilmaz A, Ulusoy RE, Kardesoglu E, et al. Short QT interval syndrome: a case report. J Electrocardiol 2005;38:371–374.
20. Lu LX, Zhou W, Zhang X, et al. Short QT syndrome: a case report and review of literature. Resuscitation 2006;71:115–121.
21. Mizobuchi M, Enjoji Y, Yamamoto R, et al. Nifekalant and disopyramide in a patient with short QT syndrome: evaluation of pharmacological effects and electrophysiological properties. Pacing Clin Electrophysiol 2008;31:1229–1232.
22. Schimpf R, Wolpert C, Bianchi F, et al. Congenital short QT syndrome and implantable cardioverter defibrillator treatment: inherent risk for inappropriate shock delivery. J Cardiovasc Electrophysiol 2003;14:1273–1277.
23. Viskin S, Zeliser D, Ish-Shalom M, et al. Is idiopathic ventricular fibrillation a short QT syndrome? Comparison of QT intervals of patients with idiopathic ventricular fibrillation and healthy controls. Heart Rhythm 2004;1:587–591.
24. Redpath CJ, Green MS, Birnie DH, et al. Rapid genetic testing facilitating the diagnosis of short QT syndrome. Can J Cardiol 2009;25:e133–e135.
25. Villafane J, Young ML, Maury P, et al. Short QT syndrome in a pediatric patient. Pediatr Cardiol 2009;30:846–850.
26. Anttonen O, Junttila MJ, Maury P, et al. Differences in twelve-lead electrocardiogram between symptomatic and asymptomatic subjects with short QT interval. Heart Rhythm 2009;6:267–271.
27. Peters S, Selbig D. Early repolarization phenomenon in arrhythmogenic right ventricular dysplasia-cardiomyopathy and sudden cardiac arrest due to ventricular fibrillation. Europace 2008;10:1447–1449.
28. Sato A, Furushima H, Hosaka Y, et al. Frequency and characteristics of J-wave. Jpn J Electrocardiol 2009;29(Suppl 3):304.
29. Mehta M, Jain AC, Mehta A. Early repolarization. Clin Cardiol 1999;22:59–65.
30. Hayashi M, Murata M, Satoh M, et al. Sudden nocturnal death in young males from ventricular flutter. Jpn Heart J 1985;26:585–591.
31. Otto CM, Tauxe RV, Cobb LA, et al. Ventricular fibrillation causes sudden death in Southeast Asian immigrants. Ann Intern Med 1984;101:45–47.
32. Garg A, Finneran W, Teld GK, Familial sudden cardiac death associated with a terminal QRS abnormality on surface 12-lead electrocardiogram in the index case. J Cardiovasc Electrophysiol 1998;9:642–647.
33. Letsas KP, Sacher F, Probst V, et al. Prevalence of early repolarization pattern in inferolateral leads in patients with Brugada syndrome. Heart Rhythm 2008; 5:1685–1689.
34. Kamakura S, Ohe T, Nakazawa K, et al. Long-term prognosis of probands with Brugada-pattern ST elevation in V1-V3 leads. Circ Arrhythmia Electrophysiol 2009;2:495–503.
35. Viskin S, Lesh MD, Eldar M, et al. Mode of onset of malignant ventricular arrhythmias in idiopathic ventricular fibrillation. J Cardiovasc Electrophysiol 1997;8:1115–1120.
36. Nam GB, Ko KH, Kim J, et al. Mode of onset of ventricular fibrillation in patients with early repolarization pattern vs. Brugada syndrome. Eur Heart J 2010;31:330–339.
37. Haissaguerre M, Sacher F, Nogami A, et al. Characteristics of recurrent ventricular fibrillation associated with inferolateral early repolarization role of drug therapy. J Am Coll Cardiol 2009;53:612–619.
38. Extramiana F, Antzelevitch C. Amplified transmural dispersion of repolarization as the basis for arrhythmogenesis in a canine ventricular-wedge model of short QT syndrome. Circulation 2004;110:3661–3666.
39. Shimizu W, Antzelevitch C. Sodium channel block with mexiletine is effective in reducing dispersion of repolarization and preventing torsade de pointes in LQT2 and LQT3 models of the long QT syndrome. Circulation 1997;96:2038–2047.
40. Spach MS, Barr RC, Benson W, et al. Body surface low-level potentials during ventricular repolarization with analysis of the ST segment: variability in normal subjects. Circulation 1979;59:822–836.
41. Hashiba K, Hereditary QT prolongation syndrome in Japan: genetic analysis and pathological findings of the conducting system. Jpn Circ J 1978;42:1133–1150.
42. Makkar RR, Fromm BS, Steinman RT, et al. Female gender as a risk factor for torsades de pointes associated with cardiovascular drugs. JAMA 1993;270: 2590–2597.
43. Shimizu W, Matsuo K, Kokubo Y, et al. Sex hormone and gender difference. Role of testosterone on male predominance in Brugada syndrome. J Cardiovasc Electrophysiol 2007;18:415–421.
44. Furukawa T, Kurokawa J. Regulation of cardiac ion channels via non-genomic action of sex steroid hormones: implication for the gender difference in cardiac arrhythmias. Pharmacol Ther 2007;115:106–115.
45. Bigi MA, Aslani A, Short QT interval: a novel predictor of androgen abuse in strength trained athletes. Ann Noninvas Electrocardiol 2009;14:35–39.
46. Charbit B, Christin-Maitre S, Demolis JL, et al. Effects of testosterone on ventricular repolarization in hypogonadic men. Am J Cardiol 2009;103:887–890.
47. Haissaguerre M, Chatel S, Sacher F, et al. Ventricular fibrillation with prominent early repolarization associated with a rare variant of KCNJ8/KATP channel. J Cardiovasc Electrophysiol 2009;20:93–98.

KCNE2 modulation of Kv4.3 current and its potential role in fatal rhythm disorders

Jie Wu, PhD,* Wataru Shimizu, MD, PhD,† Wei-Guang Ding, MD, PhD,‡ Seiko Ohno, MD, PhD,§ Futoshi Toyoda, PhD,‡ Hideki Itoh, MD, PhD,¶ Wei-Jin Zang, MD, PhD,* Yoshihiro Miyamoto, MD, PhD,‖ Shiro Kamakura, MD, PhD,† Hiroshi Matsuura, MD, PhD,‡ Koonlawee Nademanee, MD, FACC,# Josep Brugada, MD,** Pedro Brugada, MD,†† Ramon Brugada, MD, PhD, FACC,‡‡ Matteo Vatta, PhD,§§¶¶ Jeffrey A. Towbin, MD, FAAP, FACC,§§ Charles Antzelevitch, PhD, FACC, FAHA, FHRS,‖‖ Minoru Horie, MD, PhD¶

*From the *Pharmacology Department, Medical School of Xi'an Jiaotong University, Xi'an, Shaanxi, China, †Division of Cardiology, Department of Internal Medicine, National Cardiovascular Center, Suita, Japan, ‡Department of Physiology, Shiga University of Medical Science, Ohtsu, Japan, §Department of Cardiovascular Medicine, Kyoto University of Graduate School of Medicine, Kyoto, Japan, ¶Department of Cardiovascular Medicine, Shiga University of Medical Science, Shiga, Japan, ‖Laboratory of Molecular Genetics, National Cardiovascular Center, Suita, Japan, #Department of Medicine (Cardiology), University of Southern California, Los Angeles, California, **Cardiovascular Institute, Hospital Clinic, University of Barcelona, Barcelona, Spain, ††Heart Rhythm Management Centre, Free University of Brussels (UZ Brussel) VUB, Brussels, Belgium, ‡‡School of Medicine, Cardiovascular Genetics Center, University of Girona, Girona, Spain, §§Departments of Pediatrics, Baylor College of Medicine, Houston, Texas, ¶¶Department of Molecular Physiology and Biophysics, Baylor College of Medicine, Houston, Texas, and ‖‖Masonic Medical Research Laboratory, Utica, New York.*

BACKGROUND The transient outward current I_{to} is of critical importance in regulating myocardial electrical properties during the very early phase of the action potential. The auxiliary β subunit *KCNE2* recently was shown to modulate I_{to}.

OBJECTIVE The purpose of this study was to examine the contributions of *KCNE2* and its two published variants (M54T, I57T) to I_{to}.

METHODS The functional interaction between Kv4.3 (α subunit of human I_{to}) and wild-type (WT), M54T, and I57T *KCNE2*, expressed in a heterologous cell line, was studied using patch-clamp techniques.

RESULTS Compared to expression of Kv4.3 alone, co-expression of WT *KCNE2* significantly reduced peak current density, slowed the rate of inactivation, and caused a positive shift of voltage dependence of steady-state inactivation curve. These modifications rendered Kv4.3 channels more similar to native cardiac I_{to}. Both M54T and I57T variants significantly increased I_{to} current density and slowed the inactivation rate compared with WT *KCNE2*. Moreover, both variants accelerated the recovery from inactivation.

CONCLUSION The study results suggest that *KCNE2* plays a critical role in the normal function of the native I_{to} channel complex in human heart and that M54T and I57T variants lead to a gain of function of I_{to}, which may contribute to generating potential arrhythmogeneity and pathogenesis for inherited fatal rhythm disorders.

KEYWORDS Cardiac arrhythmia; M54T variation; I57T variation; *KCNE2*; Kv4.3; Sudden cardiac death

ABBREVIATIONS CHO = Chinese hamster ovary; **HERG** = human ether-a-go-go related gene; **WT** = wild type

(Heart Rhythm 2010;7:199–205) © 2010 Heart Rhythm Society. Published by Elsevier Inc. All rights reserved.

Introduction

Classic voltage-gated K^+ channels consist of four pore-forming (α) subunits that contain the voltage sensor and ion selectivity filter[1,2] and accessory regulating (β) subunits.[3] *KCNE* family genes encode several kinds of β subunits consisting of single transmembrane-domain peptides that co-assemble with α subunits to modulate ion selectivity, gating kinetics, second messenger regulation, and the pharmacology of K^+ channels. Association of the *KCNE1* product minK with the α subunit Kv7.1 encoding *KCNQ1* forms the slowly activating delayed rectifier K^+ current I_{Ks} in the heart.[4,5] In contrast, association of the *KCNE2* product MiRP1 with the human ether-a-go-go related gene (HERG) forms the cardiac rapid delayed rectifier K^+ current I_{Kr}.[6]

The first two authors contributed equally to the original concept and the authorship of this study. This study was supported by grants from the Ministry of Education, Culture, Sports, Science, Technology Leading Project for Biosimulation to Dr. Horie; Health Sciences Research grants (H18-Research on Human Genome-002) from the Ministry of Health, Labour and Welfare, Japan to Drs. Shimizu and Horie; the National Natural Science Foundation of China (Key Program, No.30930105; General Program, No. 30873058, 30770785) and the National Basic Research Program of China (973 Program, No. 2007CB512005) and CMB Distinguished Professorships Award (No. F510000/G16916404) to Dr. Zang; and National Institutes of Health Grant HL47678 and Free and Accepted Masons of New York State and Florida to Dr. Antzelevitch. **Address reprint requests and correspondence:** Dr. Minoru Horie, Department of Cardiovascular and Respiratory Medicine, Shiga University of Medical Science, Otsu, Shiga 520-2192, Japan. E-mail address: horie@belle.shiga-med.ac.jp. (Received August 20, 2009; accepted October 7, 2009.)

1547-5271/$ -see front matter © 2010 Heart Rhythm Society. Published by Elsevier Inc. All rights reserved. doi:10.1016/j.hrthm.2009.10.012

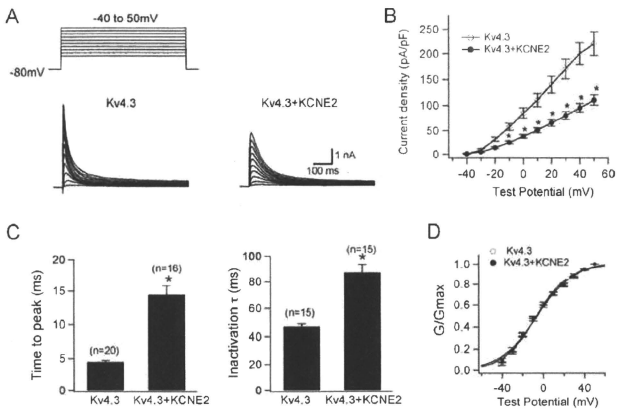

Figure 1 *KCNE2* co-expression with Kv4.3 produces smaller I_{to}-like currents with slower activation/inactivation kinetics. **A:** Representative current traces recorded from Chinese hamster ovary (CHO) cells expressing Kv4.3 **(left)** and Kv4.3 + *KCNE2* **(right)**. As shown in the **inset** in panel A, depolarizing step pulses of 1-second duration were introduced from a holding potential of −80 mV to potentials ranging from −40 to +50 mV in 10-mV increments. **B:** Current–voltage relationship curve showing peak current densities in the absence and presence of co-transfected *KCNE2* (*P <.05 vs Kv4.3). **C:** Bar graphs showing the kinetic properties of reconstituted channel currents: time to peak of activation course **(left)** and inactivation time constants **(right)** measured using test potential to +20 mV (*P <.05 vs Kv4.3). Numbers in parentheses indicate numbers of experiments. **D:** Normalized conductance–voltage relationship for peak outward current of Kv4.3 and Kv4.3 + *KCNE2* channels.

Abbott et al reported that three *KCNE2* variants (Q9E, M54T, I57T) caused a loss of function in I_{Kr} and thereby were associated with the congenital or drug-induced long QT syndrome.[6,7] However, the reported QTc values in two index patients with M54T and I57T variants, both located in the transmembrane segment of MiRP1, were only mildly prolonged (390–500 ms and 470 ms).[6] We recently identified the same missense *KCNE2* variant, I57T, in which isoleucine was replaced by threonine at codon 57, in three unrelated probands showing a Brugada type 1 ECG. These findings are difficult to explain on the basis of a loss of function in I_{Kr}, thus leading us to explore other mechanisms.

Recent studies have demonstrated that interaction between α and β subunits (*KCNEs*) of voltage-gated K^+ channel is more promiscuous; for example, MiRP1 has been shown to interact with Kv7.1,[8–10] HCN1,[11] Kv2.1,[12] and Kv4.2.[13] These studies suggest that MiRP1 may also co-associate with Kv4.3 and contribute to the function of transient outward current (I_{to}) channels.[14] Indeed, a recent study reported that I_{to} is diminished in *kcne2* (–/–) mice.[15]

In the human heart, I_{to} currents are of critical importance in regulating myocardial electrical properties during the very early phase of the action potential and are thought to be central to the pathogenesis of Brugada-type ECG manifestations.[16] Antzelevitch et al demonstrated that a gain of function in I_{to} secondary to a mutation in *KCNE3* contributes to a Brugada phenotype by interacting with Kv4.3 and thereby promoting arrhythmogenicity.[14]

We hypothesized that mutations in *KCNE2* may have similar actions and characterize the functional consequences of interaction of wild-type (WT) and two mutant (I57T, M54T) MiRP1 with Kv4.3[17,18] using heterologous co-expression of these α and β subunits in Chinese hamster ovary (CHO) cells.

Methods

Heterologous expression of hKv4.3 and β subunits in CHO cells

Full-length cDNA fragment of *KCNE2* in pCR3.1 vector[10] was subcloned into pIRES-CD8 vector. This expression vector is useful in cell selection for later electrophysiologic study (see below). Two *KCNE2* mutants (M54T, I57T) were constructed using a Quick Change II XL site-directed mutagenesis kit according to the manufacturer's instructions (Stratagene, La Jolla, CA, USA) and subcloned to the same vector. Two *KCNE2* mutants were fully sequenced (ABI3100x, Applied Biosystems, Foster City, CA, USA) to ensure fidelity. Full-length cDNA encoding the short isoform of human Kv4.3 subcloned into the pIRES-GFP (Clontech, Palo Alto, CA, USA) expression vector was kindly provided by Dr. G.F. Tomaselli (Johns Hopkins University). Full-length cDNA encoding Kv channel-interacting protein (*KCNIP2*) subcloned into the PCMV-IRS expression vector was a kind gift from Dr. G.-N. Tseng (Virginia Commonwealth University). *KCND3* was transiently transfected into CHO cells together with *KCNE2* (or M54T or I57T) cDNA at equimolar ratio (*KCND3* 1.5 μg,

Table 1 Effects of *KCNE2* on Kv4.3 and Kv4.3 + KChIP2b

Parameter	Kv4.3	Kv4.3 *KCNE2*	Kv4.3 KChIP2b	Kv4.3 KChIP2b *KCNE2*
Current density at +20 mV (pA/pF)	142.0 ± 16.0 (n = 12)	66.0 ± 6.6* (n = 12)	191.5 ± 33.8 (n = 15)	77.8 ± 5.9† (n = 20)
Steady-state activation ($V_{0.5}$ in mV)	−6.5 ± 2.1 (n = 9)	−5.5 ± 1.7 (n = 11)	−7.5 ± 1.7 (n = 8)	−7.4 ± 1.4 (n = 8)
Steady-state inactivation ($V_{0.5}$ in mV)	−46.0 ± 1.3 (n = 10)	−40.8 ± 1.7* (n = 8)	−49.8 ± 1.4 (n = 7)	−44.5 ± 1.9† (n = 7)
τ of inactivation at +20 mV (τ_{inact} in ms)	47.3 ± 2.0 (n = 15)	87.2 ± 6.2* (n = 15)	47.5 ± 2.2 (n = 15)	66.6 ± 3.5† (n = 15)
Time to peak at +50 mV (TtP in ms)	4.5 ± 0.2 (n = 20)	14.4 ± 1.4* (n = 16)	4.1 ± 0.2 (n = 15)	6.1 ± 0.5† (n = 21)
τ of recovery from inactivation (ms)	419.6 ± 18.8 (n = 6)	485.6 ± 74.8 (n = 6)	89.2 ± 5.3 (n = 6)	60.2 ± 6.9† (n = 6)

*Significantly different from Kv4.3.
†Significantly different from Kv4.3 + KChIP2b.

KCNE2 1.5 μg) using Lipofectamine (Invitrogen Life Technologies, Carlsbad, CA, USA) according to the manufacturer's instructions. In one set of experiments, we also co-transfected equimolar levels of KChIP2b (*KCND3* 1.5 μg, *KCNE2* 1.5 μg, *KCNIP2* 1.5 μg). The transfected cells were then cultured in Ham's F-12 medium (Nakalai Tesque, Inc., Kyoto, Japan) supplemented with 10% fetal bovine serum (JRH Biosciences, Inc., Lenexa, KS, USA) and antibiotics (100 international units per milliliter penicillin and 100 μg/mL streptomycin) in a humidified incubator gassed with 5% CO_2 and 95% air at 37°C. The cultures were passaged every 4 to 5 days using a brief trypsin-EDTA treatment. The trypsin-EDTA treated cells were seeded onto glass coverslips in a Petri dish for later patch-clamp experiments.

Electrophysiologic recordings and data analysis

After 48 hours of transfection, a coverslip with cells was transferred to a 0.5-mL bath chamber at 25°C on an inverted microscope stage and perfused at 1 to 2 mL/min with extracellular solution containing the following (in mM): 140 NaCl, 5.4 KCl, 1.8 $CaCl_2$, 0.5 $MgCl_2$, 0.33 NaH_2PO_4, 5.5 glucose, and 5.0 HEPES; pH 7.4 with NaOH. Cells that emitted green fluorescence were chosen for patch-clamp experiments. If co-expressed with *KCNE2* (or its mutants), the cells were incubated with polystyrene microbeads precoated with anti-CD8 antibody (Dynabeads M450, Dynal, Norway) for 15 minutes. In these cases, cells that emitted green fluorescence and had attached beads were chosen for electrophysiologic recording. Whole-cell membrane currents were recorded with an EPC-8 patch-clamp amplifier (HEKA, Lambrecht, Germany), and data were low-pass filtered at 1 kHz, acquired at 5 kHz through an LIH-1600 analog-to-digital converter (HEKA), and stored on hard disk using PulseFit software (HEKA). Patch pipettes were fabricated from borosilicate glass capillaries (Narishige, Tokyo, Japan) using a horizontal microelectrode puller (P-97, Sutter Instruments, Novato, CA, USA) and the pipette tips fire-polished using a microforge. Patch pipettes had a resistance of 2.5 to 5.0 MΩ when filled with the following pipette solution (in mM): 70 potassium aspartate, 50 KCl, 10 KH_2PO_4, 1 $MgSO_4$, 3 Na_2-ATP (Sigma, Japan, Tokyo), 0.1 Li_2-GTP (Roche Diagnostics GmbH, Mannheim, Germany), 5 EGTA, and 5 HEPES (pH 7.2).

Cell membrane capacitance (C_m) was calculated from 5 mV-hyperpolarizing and depolarizing steps (20 ms) applied from a holding potential of −80 mV according to Equation 1[19]:

$$C_m = \tau_c I_0 / \Delta V_m (1 - I_\infty / I_0), \quad (1)$$

where τ_c = time constant of capacitance current relaxation, I_0 = initial peak current amplitude, ΔV_m = amplitude of voltage step, and I_∞ = steady-state current value. Whole-cell currents were elicited by a family of depolarizing voltage steps from a holding potential of −80 mV. The difference between the peak current amplitude and the current at the end of a test pulse (1-second duration) was referred to as the transient outward current. To control for cell size variability, currents were expressed as densities (pA/pF).

Steady-state activation curves were obtained by plotting the normalized conductance as a function of peak outward potentials. Steady-state inactivation curves were generated by a standard two-pulse protocol with a conditioning pulse of 500-ms duration and obtained by plotting the normalized current as a function of the test potential. Steady-state inactivation/activation kinetics were fitted to the following Boltzmann equation (Eq. 2):

$$Y(V) = 1/(1 + \exp[(V_{1/2} - V)/k]), \quad (2)$$

where Y = normalized conductance or current, $V_{1/2}$ = potential for half-maximal inactivation or activation, respectively, and k = slope factor.

Data relative to inactivation time constants, time to peak, and mean current levels were obtained by using current data recorded at +50 mV or +20 mV. Recovery from inactivation was assessed by a standard paired-pulse protocol: a 400-ms test pulse to +50 mV (P1) followed by a variable